Self-Assembling Semicrystalline Polymer into Highly Ordered, Microscopic Concentric Rings by Evaporation

Myunghwan Byun,[†] Suck Won Hong,[†] Lei Zhu,[‡] and Zhiqun Lin*,[†]

Department of Materials Science and Engineering, Iowa State University, Ames, Iowa 50011, and Polymer Program, Institute of Materials Science and Department of Chemical, Materials and Biomolecular Engineering, University of Connecticut, Storrs, Connecticut 06269

Received October 19, 2007. In Final Form: December 11, 2007

A drop of semicrystalline polymer, poly(ethylene oxide) (PEO), solution was placed in a restricted geometry consisting of a sphere on a flat substrate (i.e., sphere-on-flat geometry). Upon solvent evaporation from the sphere-on-flat geometry, microscopic concentric rings of PEO with appropriate high molecular weight were produced via controlled, repetitive pinning ("stick") and depinning ("slip") cycles of the contact line. The evaporation-induced concentric rings of PEO exhibited a fibrillar-like surface morphology. Subsequent isothermal crystallization of rings at 40 and 58 °C led to the formation of multilayer of flat-on lamellae (i.e., spiral morphology). In between adjacent spirals, depletion zones were developed during crystallization, as revealed by AFM measurements. The present highly ordered, concentric PEO rings may serve as a platform to study cell adhesion and motility, neuron guidance, cell mechanotransduction, and other biological processes.

Introduction

Drying droplets containing nonvolatile solutes (polymers, nanoparticles, single-walled carbon nanotubes, etc.) on a solid surface have been utilized to yield self-assembled, dissipative structures. These structures, including polygonal network structures (Benard cells),[1−4] fingering instabilities,[5,6] and concentric "coffee rings"[7−9] are, in general, irregular and far from equilibrium.[10] Maximum evaporative loss of solvent at the edge of the droplet triggers the accumulation of solutes and creates a local roughness; thus, the solutes transport to the edge and pin the contact line (i.e., "stick"), thereby forming a coffee ring.[7−9] The droplet then jerks (i.e., "slip") to a new position and a new coffee ring is deposited. The pinning and depinning processes alternate as solvent evaporates and, ultimately, lead to the formation of concentric coffee rings that are governed by the competition between the capillary force and the pinning force. However, since the evaporation process is usually not controlled, stochastic concentric coffee rings are formed.[7−9] Therefore, to utilize evaporation as a simple route to producing intriguing, well-ordered structures, it is essential to control the evaporation flux, the solution concentration, the interfacial interaction between the solute and substrate, etc.

We have previously demonstrated that constrained evaporation (i.e., drying in a confined geometry to provide control over the solvent evaporation and associated capillary flow) can be utilized to produce concentric rings of *amorphous* polymers and nanoparticles of high regularity over a large area in one step.[11−19] A drop of *amorphous* polymer or nanoparticle solutions was confined either between two crossed cylinders covered with single crystals of mica sheets[11] or between a spherical lens and a Si substrate (i.e., sphere-on-flat geometry), forming a capillary-held solution (i.e., capillary edge).[12−18] Experiments were performed inside a sealed chamber so that the evaporation rate of solvent was *controlled* and temperature gradient was eliminated. The evaporation in the sphere-on-flat geometry was restricted to the edge of the droplet, and the controlled, repeated stick−slip motion resulted in hundreds of concentric rings with regular spacing.[12−19]

Semicrystalline polymers, when cooled from the melt, can organize into microscopic crystalline structures (e.g., spherulites; they are optically anisotropic objects). Spherulites composed of splaying and branching thin lamellae with thickness on the order of 10 nm are often produced in thick films ($h > 1\ \mu$m),[20] where the crystallizable phase possesses a sufficient diffusivity, and thus an *edge-on* orientation is favorable (i.e., crystalline lamellae are perpendicular to the substrate).[21,22] Spiral structures, on the other hand, can be readily created in thinner films ($h < 300$ nm),

* To whom correspondence should be addressed. E-mail: zqlin@iastate.edu.

[†] Iowa State University.

[‡] University of Connecticut.

(1) Nguyen, V. X.; Stebe, K. J. *Phys. Rev. Lett.* **2002**, *88*, 164501.
(2) Maillard, M.; Motte, L.; Pileni, M. P. *Adv. Mater.* **2001**, *13*, 200.
(3) Bormashenko, E.; Pogreb, R.; Stanevsky, O.; Bormashenko, Y.; Stein, T.; Gaisin, V.-Z.; Cohen, R.; Gendelman, O. V. *Macromol. Mater. Eng.* **2005**, *290*, 114.
(4) Grigoriev, R. O. *Phys. Fluids* **2002**, *14*, 1895.
(5) Karthaus, O.; Grasjo, L.; Maruyama, N.; Shimomura, M. *Chaos* **1999**, *9*, 308.
(6) Cazabat, A. M.; Heslot, F.; Troian, S. M.; Carles, P. *Nature* **1990**, *346*, 824.
(7) Deegan, R. D.; Bakajin, O.; Dupont, T. F.; Huber, G.; Nagel, S. R.; Witten, T. A. *Nature* **1997**, *389*, 827.
(8) Deegan, R. D. *Phys. Rev. E* **2000**, *61*, 475.
(9) Deegan, R. D.; Bakajin, O.; Dupont, T. F.; Huber, G.; Nagel, S. R.; Witten, T. A. *Phys. Rev. E* **2000**, *62*, 756.
(10) Rabani, E.; Reichman, D. R.; Geissler, P. L.; Brus, L. E. *Nature* **2003**, *426*, 271.
(11) Lin, Z. Q.; Granick, S. *J. Am. Chem. Soc.* **2005**, *127*, 2816.
(12) Hong, S. W.; Xu, J.; Xia, J.; Lin, Z. Q.; Qiu, F.; Yang, Y. L. *Chem. Mater.* **2005**, *17*, 6223.
(13) Xu, J.; Xia, J.; Hong, S. W.; Lin, Z. Q.; Qiu, F.; Yang, Y. L. *Phys. Rev. Lett.* **2006**, *96*, 066104.
(14) Hong, S. W.; Giri, S.; Lin, V. S. Y.; Lin, Z. Q. *Chem. Mater.* **2006**, *18*, 5164.
(15) Hong, S. W.; Xu, J.; Lin, Z. Q. *Nano Lett.* **2006**, *6*, 2949.
(16) Hong, S. W.; Xia, J.; Byun, M.; Zou, Q.; Lin, Z. Q. *Macromolecules* **2007**, *40*, 2831.
(17) Hong, S. W.; Xia, J.; Lin, Z. Q. *Adv. Mater.* **2007**, *19*, 1413.
(18) Xu, J.; Xia, J.; Lin, Z. Q. *Angew. Chem. Int. Ed.* **2007**, *46*, 1860.
(19) Wang, J.; Xia, J.; Hong, S. W.; Qiu, F.; Yang, Y.; Lin, Z. Q. *Langmuir* **2007**, *23*, 7411.
(20) Hu, Z. J.; Baralia, G.; Bayot, V.; Gohy, J. F.; Jonas, A. M. *Nano Lett.* **2005**, *5*, 1738.
(21) Wunderlich, B. *Macromolecular Physics*; Academic Press: New York, 1976.
(22) Langer, J. S. *Rev. Mod. Phys.* **1980**, *52*, 1.

10.1021/la703270c CCC: $40.75
Published on Web 02/15/2008

where the molecular mobility is reduced, and a *flat-on* orientation is dominated (i.e., crystalline lamellae are parallel to the substrate).[21,22,28,29] Recently, polymer crystallization has been exploited to develop crystallization-enabled nanotechnology.[23,24] It is of considerable interest to study polymer crystallization confined at the micro- or nanoscale, including in ultrathin films,[25−32] semicrystalline/amorphous polymer blends,[33] dewetting of semicrystalline polymer solutions,[34−37] and semicrystalline block copolymers.[38−40] Furthermore, the use of microscopic and/or nanoscopic patterned surfaces made it possible to examine the effects of confinement on the primary nucleation, crystal morphologies, crystal growth rates, and crystal orientations of semicrystalline polymers.[41−43]

In this paper, we extend the nonvolatile solute to a *semicrystalline* polymer, i.e., poly(ethylene oxide) (PEO). The choice of PEO was motivated by its widely known crystallization and melting behavior, low melting temperature, and simple chain conformation. We demonstrate that dynamic self-assembly of semicrystalline polymers in sphere-on-flat geometry allowed the formation of periodically ordered concentric rings, which was dependent on the molecular weight of PEO and the solution concentration. The rings were micrometers wide and a few hundred nanometers high. Subsequent isothermal crystallization of PEO concentric rings at elevated temperatures (i.e., 40 and 58 °C) transformed the originally formed fibrillar-like morphology at room temperature into spiral morphology within a ring. In between adjacent spirals, depletion zones were developed during crystallization, as revealed by AFM measurements.

Experimental Section

Materials. Two PEO with different molecular weight (MW) (Sigma-Aldrich) were used in the studies. The viscosity average MWs, M_v, were 100K and 600K, denoted PEO-100K and PEO-600K, respectively. These two PEO were dissolved in acetonitrile to prepare the PEO acetonitrile solutions at different concentrations (c = 0.5 and 1.0 mg/mL). Subsequently, the solutions were purified with 0.2 μm hydrophilic membrane filters.

Sample Preparation. To construct a restricted geometry, a spherical lens and a Si wafer were used. The spherical lens made from fused silica with a radius of curvature, $R \sim 2.0$ cm, and Si substrate with [111] crystallographic orientation were cleaned by a mixture of sulfuric acid and Nonchromix. Subsequently, they were rinsed with DI water and blown dry with N_2. The sphere and Si were firmly fixed at the top and bottom of sample holders inside a sealed chamber, respectively. To implement a restricted geometry, an inchworm motor with a step motion of a few micrometers was used to place the upper sphere into contact with the lower stationary Si surface. Before they contacted (i.e., separated by approximately a few hundred micrometers apart), a drop of ~23 μL of PEO acetonitrile solutions was loaded and trapped within the gap between the sphere and Si due to the capillary force. The sphere was finally brought into contact with Si substrate by the inchworm motor such that a capillary-held PEO solution formed with the evaporation rate being highest at the extremity (Figure 1). The use of a sealed chamber eliminated the possible external influences such as the humidity in an open space and air convection.

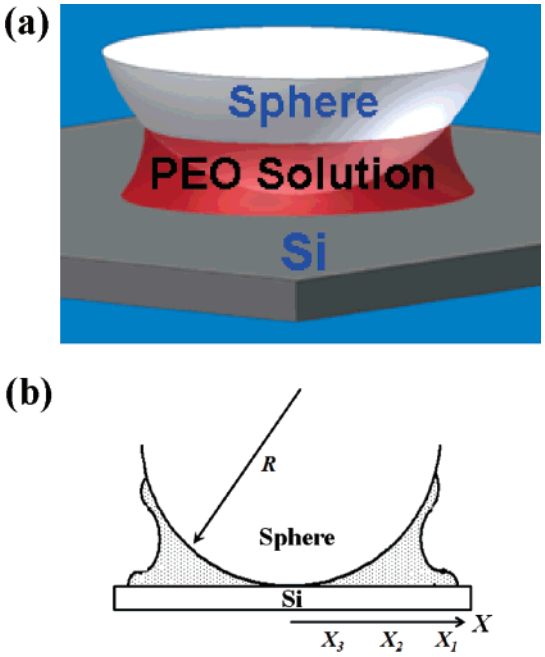

Figure 1. (a) Three-dimensional illustration of a drop of semicrystalline polymer (i.e., PEO) acetonitrile solution trapped between a sphere and a Si substrate (i.e., a sphere-on-flat geometry). (b) Cross section of the capillary-held PEO solution in part a. The radius of curvature of the upper sphere is R. The concentric rings were formed by controlled, repetitive stick−slip motion of the contact line. The distance of rings away from the sphere/Si contact center is X. (a) Ring formed at outermost region (i.e., X_1), (b) ring formed at intermediate region (i.e., X_2), and (c) ring formed at innermost region (i.e., X_3).

The evaporation took about half an hour to complete. Afterward, the sphere and Si were separated. The structures (e.g., concentric coffee rings composed of PEO) were produced on both the sphere and Si surfaces. Due to the curving effect of the sphere, only the patterns formed on Si were evaluated by the optical microscope (OM; Olympus BX51 in the reflection mode) and the atomic force microscopy [AFM; Dimension 3100 scanning force microscope in the tapping mode (Digital Instruments)]. BS-tap300 tips (Budget Sensors) with spring constants ranging from 20 to 75 N/m were used as scanning probes. Subsequently, all samples on Si substrates were transferred into a vacuum oven and kept for 12 h at room temperature to remove residual solvent from the patterns. The samples were then placed on the heat stage for isothermal annealing at a certain temperature, as described in the following. The samples were heated up to 80 °C and held at that temperature for 30 min to ensure complete melting of PEO crystals. Subsequently, the melted PEO patterns were rapidly cooled to 40 and 58 °C (below the melting temperature, T_m = 65 °C), corresponding to a high and low degree of supercooling,

(23) Li, B.; Li, C. Y. *J. Am. Chem. Soc.* **2007**, *129*, 12.
(24) Li, L.; Yang, Y.; Yang, G.; Chen, X.; Hsiao, B. S.; Chu, B.; Spanier, J. E.; Li, C. Y. *Nano Lett.* **2006**, 6.
(25) Pearce, R.; Vancso, G. J. *Macromolecules* **1997**, *30* (19), 5843.
(26) Schultz, J. M.; Miles, M. J. *J. Polym. Sci. Part B Polym. Phys.* **1998**, *36*, 2311.
(27) Chen, E. Q.; Xue, G.; Jin, S.; Lee, S. W.; Mann, I.; Moon, B. S.; Harris, F. W.; Cheng, S. Z. D. *Macromol. Rapid Commun.* **1999**, *20*, 431.
(28) Dalnoki-Veress, K.; Forrest, J. A.; Massa, M. V.; Pratt, A.; Williams, A. *J. Polym. Sci. Part B-Polym. Phys.* **2001**, *39*, 2615.
(29) Beekmans, L. G. M.; van der Meer, D. W.; Vancso, G. J. *Polymer* **2002**, *43*, 1887.
(30) Schonherr, H.; Frank, C. W. *Macromolecules* **2003**, *36*, 1188.
(31) Schonherr, H.; Frank, C. W. *Macromolecules* **2003**, *36*, 1199.
(32) Chen, E. Q.; Jing, A. J.; Weng, X.; Huang, P.; Lee, S. W.; Cheng, S. Z. D.; Hsiao, B. S.; Yeh, F. J. *Polymer* **2003**, *44*, 6051.
(33) Ferreiro, V.; Douglas, J. F.; Warren, J. A.; Karim, A. *Phys. Rev. E* **2002**, *65*, 0428021.
(34) Reiter, G. *Phys. Rev. Lett.* **2001**, *87*, 1861011.
(35) Reiter, G.; Sommer, J. U. *Phys. Rev. Lett.* **1998**, *80*, 3771.
(36) Massa, M. V.; Carvalho, J. L.; Dalnoki-Veress, K. *Phys. Rev. Lett.* **2006**, *97*, 247802.
(37) Massa, M. V.; Dalnoki-Veress, K. *Phys. Rev. Lett.* **2004**, 92.
(38) Loo, Y. L.; Register, R. A.; Ryan, A. J. *Phys. Rev. Lett.* **2000**, *84*, 4120.
(39) Reiter, G.; Castelein, G.; Sommer, J.; Röttele, A.; Thurn-Albrecht, T. *Phys. Rev. Lett.* **2001**, *87*, 226101.
(40) Chen, W. Y.; Li, C. Y.; Zheng, J. X.; Huang, P.; Zhu, L.; Ge, Q.; Quirk, R. P.; Lotz, B.; Deng, L. F.; Wu, C.; Thomas, E. L.; Cheng, S. Z. D. *Macromolecules* **2004**, *37*, 5292.
(41) Despotopoulou, M. M.; Frank, C. W.; Miller, R. D.; Rabolt, J. F. *Macromolecules* **1996**, *29*, 5797.
(42) Beers, K. L.; Douglas, J. F.; Amis, E. J.; Karim, A. *Langmuir* **2003**, *19*, 3935.
(43) Steinhart, M.; Goring, P.; Dernaika, H.; Prabhukaran, M.; Gosele, U.; Hempel, E.; Thurn-Albrecht, T. *Phys. Rev. Lett.* **2006**, *97*, 027801.

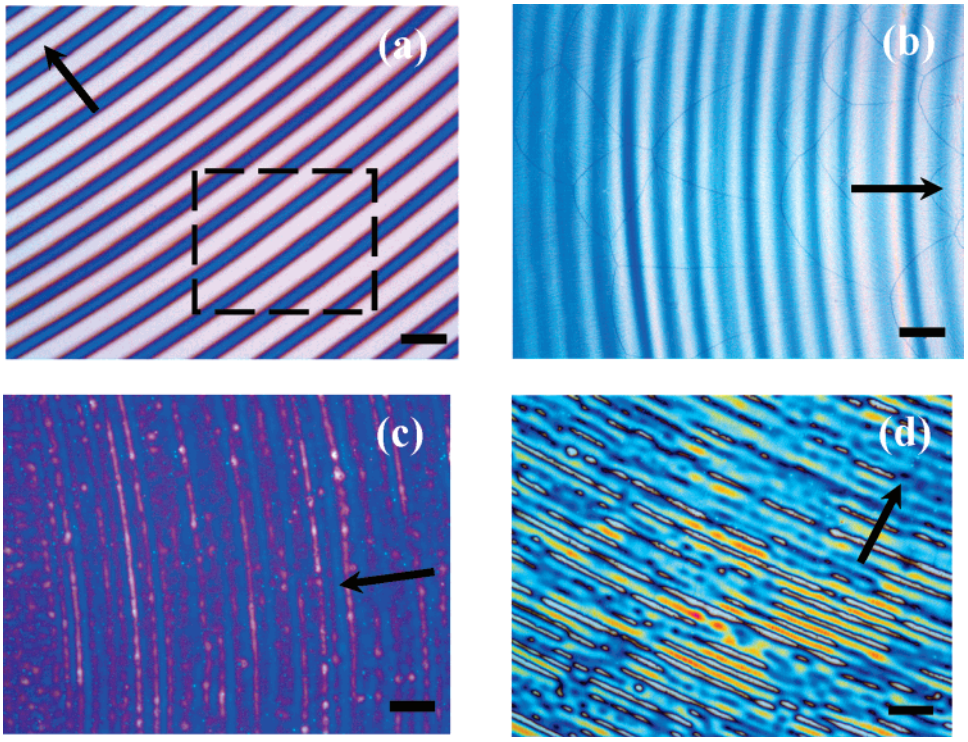

Figure 2. Optical micrographs of PEO concentric ring patterns formed at the intermediate region (i.e., X_2) from PEO-600K acetonitrile solution at (a) $c = 0.5$ mg/mL and (b) $c = 1.0$ mg/mL, respectively, and from PEO-100K acetonitrile solution at (c) $c = 0.5$ mg/mL and (d) $c = 1.0$ mg/mL, respectively. The arrow indicates the movement of the solution front toward the center of the sphere/Si contact. Scale bar = 70 μm.

respectively, and allowed to isothermally crystallize at these temperatures for 2 days. Finally, the samples were quenched to room temperature and examined by OM and AFM to evaluate the effect of crystallization temperature on the surface morphology of the concentric PEO rings.

Results and Discussion

1. Formation of Concentric Coffee Rings Composed of PEO. A semicrystalline polymer, PEO, was chosen as the nonvolatile solute due to its widely known crystallization and melting behavior, low melting temperature, and simple chain conformation. Figure 2 shows typical optical micrographs of PEO formed by drying the PEO acetonitrile solutions with different MW of PEO (PEO-100K and PEO-600K) and different solution concentrations ($c = 0.5$ and 1.0 mg/mL for both PEO-100K and PEO-600K) from a sphere-on-flat geometry (i.e., from a bound solution as shown in Figure 1). When high-MW PEO was used (i.e., PEO-600K), microscopic concentric rings of PS-600K were obtained (Figure 2a,b). It should be noted that only a small zone of the entire concentric ring pattern is shown in these images. The formation of concentric rings resulted from controlled stick−slip cycles of the contact line, that is, the competition between the pinning force (stick) and depinning force (slip) toward the sphere/Si contact center with elapsed time, as discussed in our previous work.[12,13,16−18] The Marangoni flow was suppressed in the sphere-on-flat geometry.[44,45] The solution front was arrested at the capillary edge as acetonitrile evaporated (Figure 1). The local viscosity of the contact line was then increased with time. This led to the solidification of a PEO-600K ring before the solution front jumped to the next position, where it was arrested again. Moreover, PEO is a hydrophilic molecule. The interfacial interaction between PEO and hydrophilic Si substrate is energetically favorable, thereby promoting the adsorption of PEO at the contact line. Taken together, distinct PEO rings resulted, and no PEO-600K was deposited between the rings (Figure 2a; $c = 0.5$ mg/mL). The center-to-center distance between adjacent rings, λ_{C-C}, and the height of ring, h, are 50 μm and 100 nm, respectively (Figure 2a). It is worth noting that the microscopic concentric rings composed of semicrystalline polymers with well-defined lateral dimension can be readily produced by the evaporation-induced self-assembly in sphere-on-flat geometry, which dispenses with the need for lithography and external fields. This is in contrast with the micropatterning of semicrystalline polymer solution[46] or polymer melt,[47,48] in which a micro- or nanomold (e.g., PDMS mold prepared by soft lithography[46]) was used to pattern semicrystalline polymers.

In comparison to periodic concentric rings formed in sphere-on-flat geometry (Figure 2a), highly irregular concentric rings were produced (data not shown) by allowing a drop of PEO solution to evaporate from a single surface (i.e., on a Si substrate, thereby forming an unbound droplet). The use of sphere-on-flat geometry in a sealed chamber eliminated the hydrodynamic instabilities and convection over the course of solvent evaporation (i.e., suppressing the Marangoni flow), thereby facilitating the formation of ordered structures.[12,13,16−18] In marked contrast with the distinct concentric rings observed at $c = 0.5$ mg/mL (Figure 2a), self-assembly of semicrystalline PEO from $c = 1.0$ mg/mL solution showed a connectivity between the adjacent concentric rings through the underlying continuous film (Figure 2b). The

(44) Hu, H.; Larson, R. G. *J. Phys. Chem. B* **2006**, *110*, 7090.
(45) Hu, H.; Larson, R. G. *Langmuir* **2005**, *21*, 3963.
(46) Park, Y. J.; Kang, Y. S.; Park, C. *Eur. Polym. J.* **2005**, *41*, 1002.
(47) Okerberg, B. C.; Soles, C. L.; Douglas, J. F.; Ro, H. W.; Karim, A.; Hines, D. R. *Macromolecules* **2007**, *40*, 2968.
(48) Hu, Z.; Baralia, G.; Bayot, V.; Gohy, J.-F.; Jonas, A. M. *Nano Lett.* **2005**, *5*, 1738.

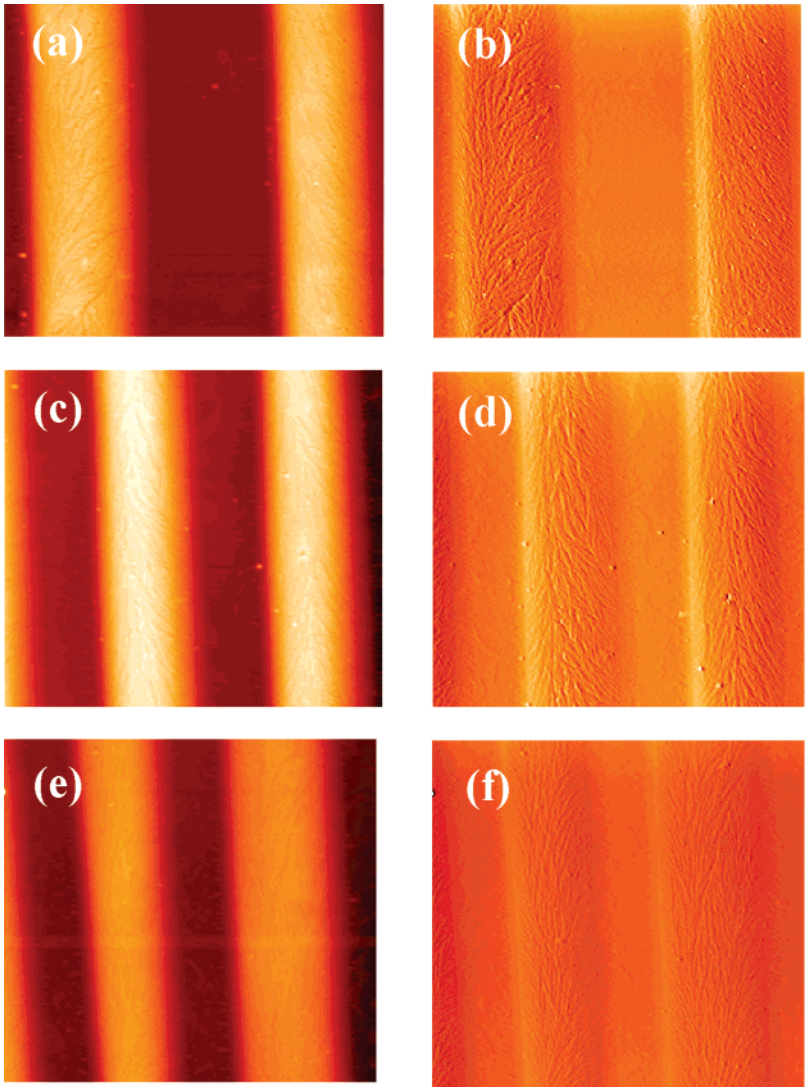

Figure 3. AFM images (height images, a, c, and e; phase images, b, d, f) of concentric rings produced from the drying-mediated self-assembly of the 0.5 mg/mL PEO-600K acetonitrile solution at room temperature. As the solution front progressed toward the sphere/Si contact center, the center-to-center distance between adjacent rings, λ_{C-C}, was reduced. (a, b) Outermost region (i.e., X_1), (c, d) intermediate region (i.e., X_2), and (e, f) innermost region (i.e., X_3). The image size is 80 × 80 μm^2.

impingement of crystals is clearly evident, represented interconnected curves superimposed on the blue background of concentric rings (Figure 2b).

Comparison of the optical micrographs of PEO surface morphologies obtained at different MW revealed that MW has a marked effect on the ring pattern formation. In the case of low-MW PEO (PEO-100K) used at both $c = 0.5$ mg/mL and 1.0 mg/mL, ringlike patterns superimposed on a continuous film were yielded. These observations suggested that the depinning force (i.e., capillary force) was not strong enough to cause the three-phase contact line to jump to a new position inward.[13] It cannot completely overcome the pinning force exerted by the deposition of PEO-100K. Thus, a rather continuous film of PEO-100K was formed. It is noteworthy that, as a model system for studying polymer crystallization, low-MW PEO with MW in the range of 1000−10 000 has been widely utilized for several decades.[49,50] Although the use of low-MW PEO generally produces pretty crystals (e.g., square-shaped crystals and finger-like crystals), in the present study no clear concentric rings were produced when it was used as the nonvolatile solute (i.e., MW < 100K).

To explore the details of polymer crystals within microscopic rings, AFM measurements were performed only on the PEO-600K rings obtained from dynamic self-assembly of the 0.5 mg/mL PEO-600K acetonitrile solution (Figure 2a). Locally, the rings appeared as parallel stripes. As the solution front moved toward the sphere/Si contact center due to evaporative loss of acetonitrile, the center-to-center distance between adjacent PEO-600K rings, λ_{C-C}, and the height of the ring, h, decreased progressively from $\lambda_{C-C} = 50.31$ μm and $h = 100.27$ nm at X_1 (Figure 3a) to $\lambda_{C-C} = 37.03$ μm and $h = 76.40$ nm at X_2 (Figure 3c) to $\lambda_{C-C} = 33.29$ μm and $h = 71.24$ nm at X_3 (Figure 3e), where X_n is the distance away from the sphere/Si contact center, as depicted in Figure 1. So it is clear that concentric PEO-600K rings were gradient in spacing and height. The measurements revealed the formation of fibrillar-like crystals (Figure 3). This contrasts with the featureless surface morphology within the ring when *amorphous* polymers were used.[13−17] The evaporative

(49) Huang, Y.; Liu, X.; Zhang, H. L.; Zhu, D. S.; Sun, Y.; Yan, S.; Wang, J.; Chen, X. F.; Wan, X. H.; Chen, E. Q.; Zhou, Q. F. *Polymer* **2006**, *47*, 1217.

(50) Cheng, S. Z. D.; Lotz, B. *Philos. Trans. R. Soc. London A* **2003**, *361*, 517.

loss of acetonitrile at the capillary edge triggered the accumulation of PEO and generated a local roughness to pin the contact line, during which PEO crystallization took place. However, due to relatively quick solvent evaporation (the boiling point of acetonitrile is 81.6 °C), PEO crystals were trapped in the metastable state, leading to the formation of PEO fibrillae inside the ring (Figure 3). Notably, PEO fibrillae were oriented, to some extent, along the rings (i.e., parallel to the edge of rings) (Figure 3b,d,f).

2. Morphological Changes of Crystallized PEO in the Ring Pattern. Isothermal annealing at 40 and 58 °C were performed only on the PEO-600K sample in which highly ordered concentric rings were obtained from the 0.5 mg/mL acetonitrile solution (Figure 2a and 3). The optical micrographs of PEO rings before and after isothermal crystallization are shown in Figure 4. Although the integrity of originally formed ring patterns (Figures 2a and 4a) was retained after annealing (Figure 4b,c), the surface topology of individual rings was altered. The fibrillar-like morphology formed from the solution state via evaporation-induced self-assembly process (Figure 4a, a closeup of Figure 2a) transformed into patch-like surface patterns (Figure 4c, a closeup of Figure 4b). In particular, AFM measurements revealed that the crystalline fibrillae tuned into multilayers of crystals (i.e., forming spiral structures), presumably formed via screw dislocation, when isothermally crystallized from the molten state to 40 °C and 58 °C, as evidenced in Figure 5. Within a spiral, the lamellar crystals were oriented parallel to the substrate (Figure 5), which is more thermodynamically stable.[49] This flat-on lamellar orientation was due to annealing-induced film thickness reduction. It is well-known that crystallization in thicker film often exhibits a spherulite morphology, consisting of lamellae that grow radially from a nucleation center.[47] As film thickness decreases, a transition to spiral structures are often resulted, due to restricted chain mobility.[26,30,31] In the present study, the average width, w, and height, h, of originally formed rings were 26.25 μm and 100.27 nm, respectively (Figure 4a). After annealing, the values changed to 28.48 μm and 67.67 nm, respectively (Figure 4b,c and Figure 5a−c), thus facilitating the spiral structure formation.

The morphology of isothermally crystallized PEO-600K at 40 and 58 °C inside the ring showed differences in the density of nucleation sites. Since high-MW PEO was used, which makes it difficult to grow into bigger crystals, the size of spiral structures (Figure 5) was small as compared to the crystals formed from low-MW counterparts. The PEO spirals are randomly dispersed within the microscopic rings. This is due to the fact that the nucleation number and sites were hard to control in polymer crystallization, and the width of microscopic ring was large, thereby imposing no confinement effect on the crystal growth. In the crystallization of polymer thin film, insufficient transport of crystallizable molecules, in general, leads to the formation of depletion zones at the crystal front.[26,30,31,35] In the present study, the depletion zones, as marked in Figure 5, were caused by the diffusion of PEO chains to the fold surfaces of the flat-on lamellae and the specific volume decrements between the melt and crystals.[51] The number of nucleation sites at 40 °C were more than that at 58 °C, which in turn resulted in more depletion zones (Figure 5d,e). High supercooling (i.e., low crystallization temperature at 40 °C) tended to activate the nucleation rate and retarded the chain diffusion rate, eventually giving rising to a considerable number of depletion zones. In contrast, low supercooling (i.e., high crystallization temperature at 58 °C) promoted a higher diffusion rate and thus formed relatively fewer nucleation sites. The root-mean-square (rms) surface roughness of PEO crystals obtained from isothermal annealing at 40 and 58 °C was 22.25 and 16.06 nm, respectively.

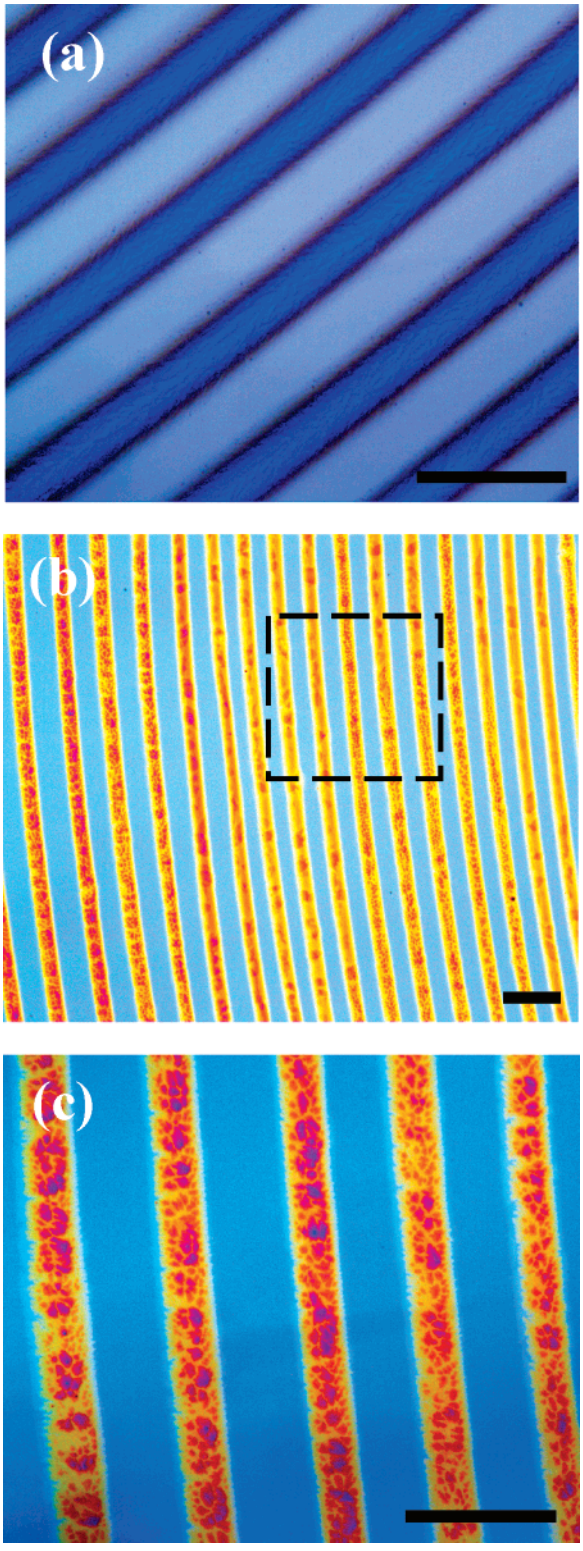

Figure 4. Optical micrographs of concentric PEO-600K rings (a) before (i.e., at room temperature) and (b, c) after isothermal crystallization at 58 °C. The PEO rings were formed from the 0.5 mg/mL PEO-600K acetonitrile solution. Optical micrographs a and c are the close-ups of the black boxes in Figures 2a and 4b, respectively. Scale bar = 70 μm.

(51) Wang, Y.; Chan, C.-M.; Li, L.; Ng, K.-M. *Langmuir* **2006**, *22*, 7384.

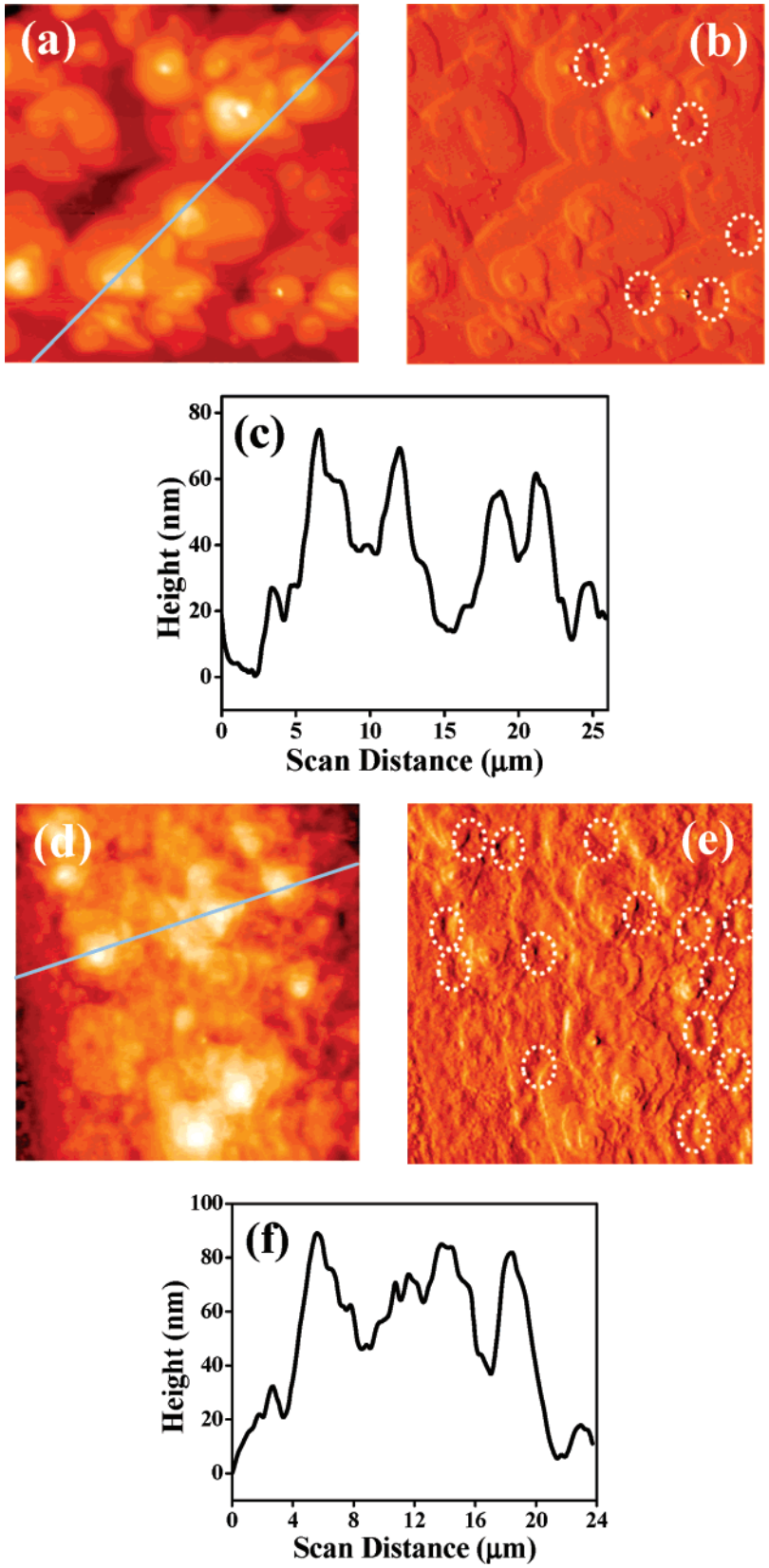

Figure 5. Surface morphologies of PEO crystals in a microscopic PEO-600K ring. (a, b) AFM height and phase images of spiral structures of PEO crystals after isothermal annealing at 58 °C. The section analysis of PEO crystal is shown in part c. (d, e) AFM height and phase images of spiral structures of PEO crystals after isothermal annealing at 40 °C. The section analysis of the PEO crystal is shown in part f. The image size is 20 × 20 μm^2.

Conclusion

The confined, axial symmetric geometry (i.e., sphere-on-flat geometry) provided a unique environment for controlling the flow within the evaporating droplet, which in turn regulated the formation of concentric rings of a semicrystalline polymer, PEO. The formation of distinct microscopic rings depended on the

MW and the solution concentration. Upon the completion of solvent evaporation, a continuous PEO thin film was left behind at low MW, while at high MW concentric PEO rings of high regularity were produced.

Subsequent isothermal crystallization of ring patterns transformed originally formed fibrillar-like PEO crystals into spirals as a result of the reduction in height of the rings by annealing. The formation of spiral terraces suggested a flat-on orientation of the lamellae. A high supercooling of PEO (corresponding to low crystallization temperature, $T = 40$ °C) generated more depletion zones than a low supercooling counterpart ($T = 58$ °C). We envisage that, by applying the upper spherical lens with a larger radius of curvature,[16] concentric rings of PEO with much smaller width (a few micron or submicron) and height (tens of nanometers or a few nanometers) could be produced in such a dimension that is comparable to the lateral size of a PEO spiral. Thus, hierarchically ordered structures may be anticipated, in which only a single row of PEO spirals are allowed to form, and they are adjacent to one another, residing along the ring in a concentric ring mode. Since the confinement imposed by the ring width may dramatically affect the nucleation and growth of crystals, crystal morphology, and crystal orientation, some intriguing surface morphologies other than spirals may also form. This work is currently under investigation. PEO is a biocompatible polymer suitable for biological application, since surfaces covered with PEO have shown to be nonantigenic, nonimmunogenic, and protein resistant.[52] Therefore, the present highly ordered concentric PEO rings may serve as a platform to study cell adhesion and motility, neuron guidance, cell mechanotransduction, and other biological processes.[53,54]

Acknowledgment. We gratefully acknowledge support from the National Science Foundation (CBET-0730611) and the 3M non-tenured faculty award. We also thank Qingze Zou for use of AFM.

LA703270C

(52) Nikolic, M. S.; Krack, M.; Aleksandrovic, V.; Kornowski, A.; Forster, S.; Weller, H. *Angew. Chem. Int. Ed.* **2006**, *45*, 6577.
(53) Chen, X.; Hirtz, M.; Fuchs, H.; Chi, L. *Langmuir* **2007**, 23.
(54) Kumar, G.; Ho, C. C.; Co, C. C. *Adv. Mater.* **2007**, *19*, 1084.